HHS Public Access

Author manuscript

J Immunol Methods. Author manuscript; available in PMC 2022 July 01.

Published in final edited form as:

J Immunol Methods. 2022 July ; 506: 113290. doi:10.1016/j.jim.2022.113290.

Combined analysis of T cell activation and T cell-mediated cytotoxicity by imaging cytometry

Monica K. Chanda[a,b,1],

Claire E. Shudde[a,1],

Taylor L. Piper[a],

Yating Zheng[a],

Adam H. Courtney[a,b,c,*]

[a]Department of Pharmacology, University of Michigan Medical School, Ann Arbor, MI 48109, United States of America

[b]Cancer Biology Graduate Program, University of Michigan Medical School, Ann Arbor, MI 48109, United States of America

[c]University of Michigan Rogel Cancer Center, Ann Arbor, MI 48109, United States of America

Abstract

Immunotherapies for the treatment of cancer have spurred the development of new drugs that seek to harness the ability of T cells to recognize and kill malignant cells. There is a substantial need to evaluate how these experimental drugs influence T cell functional outputs in co-culture systems that contain cancerous cells. We describe an imaging cytometry-based platform that can simultaneously quantify activated T cells and the capacity of these T cells to kill cancer cells. Our platform was developed using the Nur77-GFP reporter system because GFP expression provides a direct readout of T cell activation that is induced by T cell antigen receptor (TCR) signaling. We combined the Nur77-GFP reporter system with a cancer cell line that displays a TCR-specific antigen and evaluated the relationship between T cell activation and cancer cell death. We demonstrate that imaging cytometry can be used to quantify the number of activated cytotoxic CD8+ T cells (CTLs) and the capacity of these CTLs to recognize and kill adherent MC38 cancer cells. We tested whether this platform could evaluate heterogenous lymphocyte populations by quantifying the proportion of antigen-specific activated T cells in co-cultures that contain unresponsive lymphocytes. The effects of a SRC family kinase inhibitor on CTL activation

*Corresponding author at: Department of Pharmacology, University of Michigan Medical School, Ann Arbor, MI 48109, United States of America. adamhc@umich.edu (A.H. Courtney).

[1]equal contribution.

Author contributions

AHC, MKC, CES conceived and designed the project. Experiments were performed by MKC, CES, TLP, and YZ. The data were analyzed and interpreted by AHC, MKC, CES, and TLP. The manuscript was prepared by AHC, MKC, CES, and TLP. All authors reviewed and edited the manuscript.

Appendix A. Supplementary data

Supplementary data to this article can be found online at https://doi.org/10.1016/j.jim.2022.113290.

Declaration of Competing Interest

The authors declare no competing interests.

and MC38 cell death were also determined. Our findings demonstrate that the Nur77-GFP reporter system can be used to evaluate the effects of diverse treatment conditions on T cell-cancer co-cultures in a microtiter plate-based format by imaging cytometry. We anticipate the combined analysis of T cell activation with T cell-mediated cancer cell death can be used to rapidly assess immuno-oncology drug candidates and T cell-based therapeutics.

Keywords

T cell activation; T cell-mediated cytotoxicity; Imaging cytometry; Immuno-oncology; Cancer; Nur77-GFP

1. Introduction

Immunotherapies have revolutionized cancer treatment by harnessing the ability of T cells to target and kill malignant cells (Chen and Mellman, 2013). These successes have led to the development of new immuno-oncology treatment strategies (Upadhaya et al., 2020). Accordingly, there is an expanded need to evaluate how treatment strategies and potential drug targets affect interactions between T cells and cancer cells by ex vivo co-culture systems. Plate-based co-cultures that combine T cells and cancer cells can be used to assess the killing of cancer cells by cytotoxic T cells (CTLs). These assays generally rely on indirect readouts of cell death, such as the release of intracellular contents, which includes lactate dehydrogenase (LDH) or chromium (^{51}Cr) (Korzeniewski and Callewaert, 1983; Miller and Dunkley, 1974). Although these indirect readouts correlate with cell death, they require the use of radioactive isotopes or enzymatic substrates to quantify the relative amount of cell death in each sample. Fluorescent membrane impermeable dyes can be used to label intracellular contents, such as nucleic acids, that become accessible when cell death results in a loss of membrane integrity. Quantification of dead cell numbers can be performed by imaging and flow cytometry using dyes, such as propidium iodide (PI) (Chan et al., 2011; Piriou et al., 2000). Although methods such as LDH release and PI staining can be used to assess cell death, their utility in T cell-cancer co-culture systems can be limited by a lack of insight into the activation status of T cells. This consideration is particularly relevant because prior to killing a cancer cell, a T cell must recognize and become activated by a tumor antigen (Jenkins et al., 2009).

A T cell can become activated by peptide-major histocompatibility complexes (pMHC) found on the surface of an adjacent cell. These pMHC ligands are recognized by the T cell antigen receptor (TCR) which, upon binding to an antigenic agonist, causes the signaling events needed for T cell activation to occur (Courtney et al., 2018; Davis and Bjorkman, 1988). T cell activation results in changes in transcription, metabolism, and other pathways necessary for a T cell response. However, this response may not be uniform across a population of T cells. The extent to which cytotoxic T cells recognize and kill cancerous cells can be influenced by phenotypic heterogeneity within the T cell population. Such T cell heterogeneity can be found within populations of tumor infiltrating lymphocytes (TILs) (Oja et al., 2018), but can also be introduced by ex vivo T cell expansion, differentiation, and transduction procedures (Piscopo et al., 2018), or by genetic modification with CRISPR/

Cas9 (Rupp et al., 2017). Therefore, to interpret how observed differences in cell death arise in mixed co-culture systems, the extent of T cell activation is a critical consideration.

The analysis of activated T cell populations in mixed cell cultures has generally been determined by labeling cells with fluorescent antibodies that are specific for activation markers found on the T cell surface followed by quantification using flow cytometry (Caruso et al., 1997; Maino et al., 1995). More recently, the Nur77-GFP reporter system has been utilized because it provides a robust readout of TCR signaling-mediated activation of T cells (Moran et al., 2011; Zikherman et al., 2012). GFP expression occurs when the immediate-early gene encoding Nur77 (*Nr4a1*) becomes upregulated following TCR engagement (Osborne et al., 1994). Because flow cytometry requires cellular suspensions, it is limited by sample processing requirements and throughput. These considerations create a barrier to the use of flow cytometric analysis for microtiter plate-based analyses of mixed co-culture systems containing both T cells and the adherent cancerous cells they can potentially recognize. Imaging cytometry can address these limitations because it does not require the sample to be processed to yield a cell suspension. Moreover, imaging is more rapid and nondestructive, which can allow samples to be imaged repeatedly over time. Morphological changes can also be observed and absolute cell counts can be obtained.

Imaging cytometry methods have been developed to evaluate T cell-mediated cytotoxicity (Chan et al., 2019; Maldini et al., 2020). These studies incorporated a fluorescent protein (GFP) that was released by cancer cells following cell death. This fluorescent readout was used to quantify cancer cell death mediated by T or NK cells in co-cultures by assessing the number of viable GFP+ cells. Imaging cytometry provides a rapid readout of cancer cell death compatible with microtiter plate-based co-culture systems, but methods are needed that provide an integrated, direct readout of the activated T cells that mediate this process. Because of potential T cell heterogeneity, it is often necessary to determine the proportion of activated T cells that mediate a functional response. For example, receptor-targeting drugs, such as co-stimulatory agonists, may act on a specific subpopulation of T cells if expression of the targeted receptor is restricted to a T cell subset. We anticipated that methods to assess cell death by imaging cytometry could be combined with reporters of T cell activation, such as Nur77-GFP. In this way, the proportion of activated T cells responsible for mediating a functional output, such as cancer cell death, can be determined by imaging cytometry-based assays.

The Nur77-GFP reporter is upregulated within several hours following stimulation by an antigenic TCR agonist. In comparison to activation markers, such as CD69, it is a more faithful readout of TCR-mediated activation because its upregulation is less sensitive to inflammatory or mitogenic signals, such as those caused by cytokines (Ashouri and Weiss, 2017). Accordingly, the Nur77-GFP reporter system can be used to assess antigen-induced activation of T cells by both in vivo and ex vivo systems (Au-Yeung et al., 2014; Courtney et al., 2019; Moran et al., 2016). We sought to determine whether the Nur77-GFP reporter could be used to quantify activated T cells by imaging cytometry and to test its utility in mixed co-culture systems. Our goal was to monitor populations of activated T cells that mediate the targeted killing of cancer cells. We combined Nur77-GFP CTLs with cancer cells that displayed an antigenic agonist. We determined that both the proportion of activated

T cells, based on their expression of GFP, and the extent of cancer cell death could be quantified by imaging cytometry. Our results indicate that this platform provides a robust, integrated readout of T cell activation and cancer cell death in heterogenous co-culture systems.

2. Methods

2.1. Mice and cell lines

All mice were bred and maintained on the C57BL/6 genetic background. The Nur77-GFP reporter has been previously described (Moran et al., 2011; Zikherman et al., 2012). Nur77-GFP transgenic mice were crossed to OT-I TCR transgenic mice (Hogquist et al., 1994). For all experiments, mice were used between 6 and 12 weeks of age. All animals were housed at U-M in a specific-pathogen-free (SPF) facility and were treated according to protocols that were approved by U-M animal care ethics and veterinary committees and are in accordance with NIH guidelines. Lenti-X 293T (LX293T) cells were obtained from Takara. MC38 cells were generously provided by Dr. Weiping Zou (University of Michigan). Cells were maintained in a tissue culture incubator at 37 °C with 5% CO_2 in culture medium. Adherent cell lines were maintained in DMEM supplemented with 10% fetal bovine serum and 2 mM glutamine.

2.2. Reagents

Chemicals: PP2 inhibitor (Tocris), propidium iodide (PI) and Hoechst stains (Biolegend), LT-1 transfection reagent (Mirus). For imaging analysis, #0030730119 (tissue culture (TC) treated) and #0030730011 (non-TC culture treated) Eppendorf 96-well plates were used. Non-TC treated plates were used for agonistic antibody adsorption. Sterile carrier-free anti-CD3 (2C11) and anti-CD28 (37.51) were obtained from Biolegend. Fluorescent anti-TCRβ (AF647) (H57–597) and anti-CD8α (PE) (53–6.7) were obtained from Biolegend. Streptavidin nanospheres were obtained from Biolegend (#480016). Biotinylated antibodies used for negative selection cocktail were obtained from Biolegend: Biotin anti-CD11b (M1/70) (#101204), Biotin anti-CD11c (N418) (#117304), Biotin anti-CD19 (6D5) (#115504), Biotin anti-CD24 (M1/69) (#101804), Biotin anti-CD45R (B220) (RA3-6B2) (#103204), Biotin anti-CD49b (DX5) (#108904), Biotin anti-TER119 (clone TER-119) (#116204), Biotin CD4 (GK1.5) (#100404). Antibodies (0.5 mg each, except for 0.1 mg anti-CD11c) were pooled and dialyzed in PBS before sterile filtration and storage at 80 °C.

2.3. Plasmids

The gene encoding the full-length Ovalbumin protein was ordered as a synthetic gene fragment (IDT). BP Clonase II (ThermoFisher #11789020) was used to insert the gene into a pDONR221 plasmid (ThermoFisher #12536017). PCR mutagenesis was used to remove the N-terminal secretion sequence (Diebold et al., 2001). The resulting plasmid was linearized by PCR and HiFi DNA assembly (NEB #E2621) was used to insert an IRES sequence followed by iRFP713 (obtained from Addgene #31857) (Fig. S1). The pDONR plasmid was combined with the pLEX307 destination vector obtained from Addgene (#41392) and the insert transferred using LR Clonase II (ThermoFisher #11791020). The resulting pLEX307 OVA IRES iRFP713 plasmid was used to generate cell lines by viral transduction. The

pMD2.G (#12259) plasmid was obtained from Addgene. The pCMV dR8.91 plasmid was generously provided by the Lim laboratory (UCSF).

2.4. MC38-OVA cell line

Viral supernatants were prepared by transfecting LX293T cells with pLEX307 OVA IRES iRFP713, pMD2.G, and pCMV dR8.91 plasmids. LX293T cells were plated out in 2 mL of culture medium onto 6-well plates the day prior. Transfection and virus production were performed according to protocols provided by the Broad Institute TRC/GPP (https://portals.broadinstitute.org/gpp/public/) (Root et al., 2006). LX293T cells were between 70 and 80% confluency the day of transfection. pLEX307 OVA IRES iRFP713 (0.5 μg/well), pMD2.G (0.05 μg/well), and pCMV dR8.91 (0.5 μg/well) were diluted into Opti-MEM medium and combined with Mirus LT-1 transfection reagent (#MIR2306). The plasmids and LT-1 reagent were incubated for 30 min at room temperature and then added directly to LX293T cells drop-wise. The following day culture medium was replaced with 2 mL of DMEM supplemented with 20% FBS and glutamine. The next day the culture medium containing the virus was collected and centrifuged to pellet any dislodged LX293T cells. The viral supernatant was then filtered (0.45 μm) to remove residual cells. Viral supernatants were collected the same day as MC38 transduction was performed. MC38 cells were plated out in 2 mL of culture medium in 6-well plates (200,000 cells/well). The following day 1 mL of viral supernatant was added per well. The medium was replaced after 1–2 days. Following 3–4 days in culture, fluorescence activated cell sorting (FACS) was used to seed cells into 96-well plates (1 cell per well) using an Invitrogen Bigfoot Spectral Cell Sorter (ThermoFisher). Several clones were obtained and directly compared by the T cell-mediated cytotoxicity assay (Fig. S2). Individual clones were isolated and analyzed for iRFP713 expression by flow cytometry (Fig. S3). A single clone, 2E7, was used for all further experiments described. The MC38-OVA (2E7) cell line will be made available upon request.

2.5. T cell activation by agonistic antibodies

Agonistic antibodies were diluted with sterile PBS and each well of a non-TC treated 96-well plate was coated with a volume of 50 μL for approximately 16 h at 4 °C. Wells were rinsed twice with PBS prior to addition of T cells in complete MEM medium (phenol red-free MEM supplemented with 10% FBS, 2 mM glutamine, non-essential amino acids, penicillin and streptomycin, 1 mM sodium pyruvate, 50 μM 2-mercaptoethanol, and 10 mM HEPES). Complete MEM was used to reduce background fluorescence caused by riboflavin, which is present in RPMI and DMEM at a greater concentration. CD8+ T cells were purified by negative selection as previously described (Au-Yeung et al., 2017). Briefly, spleen and lymph nodes were isolated from a Nur77-GFP mouse and ruptured in complete medium. T cells were washed and resuspended in FACS buffer (PBS supplemented with 2% FBS and 1 mM EDTA) at 10^8 cells per mL. Rat serum (75 μL per mL) obtained from Jackson ImmunoResearch (#012-000-120) was added, followed by a biotinylated antibody cocktail (30 μL per mL). Cells were incubated for 10 min at room temperature and then FACS buffer added to a volume of 10 mL. Cells were pelleted and supernatant removed by aspiration. Cells were resuspended in FACS buffer at 10^8 cells per mL before addition of 90 μL per mL of streptavidin nanospheres (Biolegend #480016). The sample was gently mixed and incubated for 5 min and additional FACS buffer added if necessary to ensure a minimum

volume of 5 mL. The sample was placed in a magnet for 5 min and negatively selected cells isolated by decanting into a fresh tube. Cells isolated by this approach and analyzed by flow cytometry are typically ~90–94% CD8+ TCRβ+ (Fig. S4). Purified T cells were pelleted and resuspended in complete MEM at 4×10^5 cells per mL. To each well of the 96-well plate, 50 uL of the T cell suspension was added (20,000 cells) and cultured overnight for 16 h. The following day nuclei were labeled by adding 100 uL of PBS containing Hoechst dye (20 μM) to each well. Plates were incubated for 30 min and then imaged using a Nexcelom Celigo imaging cytometer.

2.6. CD8+ effector T cells

Splenocytes were isolated from an OT-I Nur77-GFP mouse by rupturing the spleen in complete RPMI medium (RPMI supplemented with 10% FBS, 2 mM glutamine, non-essential amino acids, penicillin and streptomycin, 1 mM sodium pyruvate, 50 uM 2-mercaptoethanol, and 10 mM HEPES). The isolated cells were washed and 3×10^6 cells were plated out in 3 mL of complete RPMI supplemented with 10 ng/mL of recombinant mouse IL-2 (Peprotech #212–12). A peptide recognized by the OT-I TCR was added. For these studies, 20 nM of the SIIQFERL (Q4R7) variant of Ovalbumin (257–264) was used. The Q4R7 peptide was custom synthesized by Genescript. Similar results have been obtained using 20 nM of the WT SIINFEKL peptide (Genescript #RP10611). After 2 days of culture, small clumps of proliferating T cells should be observed. An additional 2 mL of medium containing IL-2 was added to each well. On day 3, substantial proliferation with large clumps of cells should be observed. Cells were counted and passaged to maintain a density of less than 2×10^6 cells per mL. After 4 days of expansion, the culture should contain only CD8+ Vα2+ OT-I T cells. After 4–5 days of culture, the expanded cytotoxic OT-I T cells were co-cultured with MC38-OVA cells.

2.7. T cell-cancer co-culture

MC38 and MC38-OVA cells (5,000 cells per well) were added in 50 μL of complete MEM medium (phenol red-free MEM supplemented with 10% FBS, 2 mM glutamine, non-essential amino acids, penicillin and streptomycin, 1 mM sodium pyruvate, 50 μM 2-mercaptoethanol, and 10 mM HEPES) to a 96-well plate. Plates were incubated overnight to allow cells to attach (approximately 24 h). The cancer cell number was estimated to double by the next day to 10,000 cells per well, which was used to calculated E:T ratios. The following day expanded cytotoxic CD8+ OT-I T cells (CTLs) were resuspended in complete MEM medium supplemented with IL-2 and added to the plate containing the cultured cancer cells without mixing the contents of the well (5 ng/mL IL-2). To achieve the desired effector-to-target (E:T) ratios, the number of OT-I CTLs added ranged from 50,000 (5:1) to 780 (0.078). For experiments containing decoy cells, the E:T ratio was kept constant at 0.25:1 by addition of 25 μL of OT-I T cells (2,500 cells per well) and 25 μL of splenocytes to each well. For the inhibitor-treated samples, the E:T ratio was 1:1 by addition of 50 μL of OT-I T cells (10,000 cells per well). Cells were co-cultured overnight for 16 h at 37 °C. Samples were stained by addition of 100 μL of PI (75 μM) and Hoechst (20 μM) diluted in PBS. After 30 min, the plates were centrifuged briefly to ensure cells were at the bottom of each well, and imaged on the Celigo imaging cytometer (Nexcelom). For experiments

containing decoy cells, splenocytes were combined with OT-I CTLs at varying decoy:OT-I ratios (12:1, 6:1, 3:1, 1.5:1) prior to their addition to the overnight co-culture.

2.8. T cell activation and cell-mediated toxicity measurement by imaging cytometry

The Celigo software application (V5.3) for expression analysis was used to collect brightfield and fluorescence images. A well mask was used to exclude well edges from analysis (outer 10% of each well). For T cell activation alone, the Green and Blue fluorescence channels were used to image Nur77-GFP and Hoechst respectively. For T cell-mediated cytotoxicity experiments, the Red channel was also included to image and identify PI positive cells. A mask based on Hoechst labeling was used to identify individual cells. Thresholds for identification of GFP+ and PI+ cells were set using negative controls (samples lacking antigen or agonistic antibody). Automated analysis of cell counts was performed using Celigo analysis software (V5.3) and images directly exported. Expected and total cell counts can be compared across controls and samples, as illustrated in Fig. S5. Deviations from expected cell counts occurred at higher E:T ratios, which we attributed to increased clumping of T cells around MC38-OVA cells. To account for cell death independent of T cell-mediated cytotoxicity, single cell type (monoculture) controls of MC38-OVA and CTLs were included. PI+ cells from monocultures were subtracted from PI+ counts obtained from co-cultured cells (PI+ count = PI+ co-culture − [PI+ $MC38_{only}$ + PI+ CTL_{only}]). 3–4 replicates were analyzed per sample. FCS files corresponding to each well of the plate were exported and analyzed using FlowJo software (V10.7.1) to generate depicted contour plots.

2.9. Statistical analysis

All statistical analysis was performed using GraphPad Prism software (V9.2.0).

3. Results

A readout of live activated T cells compatible with co-culture systems should provide a powerful means to evaluate experimental treatment conditions, such as immuno-oncology drug candidates. We therefore sought to determine whether the Nur77-GFP reporter could be used to quantify activated T cells by imaging cytometry. To establish feasibility, we isolated CD8+ T cells from transgenic Nur77-GFP mice by negative selection. To stimulate the TCR and induce expression of the Nur77-GFP reporter, we used an agonistic antibody that binds to CD3ε (2C11), a component of the TCR complex. The anti-CD3ε agonist was diluted to yield a range of concentrations from 0 to 12.5 μg/mL that were adsorbed onto the surface of a 96-well microtiter plate. To evaluate the effects of co-stimulation on Nur77-GFP expression, we included an anti-CD3ε dilution series that also contained a single fixed concentration (2.5 μg/mL) of an anti-CD28 co-stimulatory agonistic antibody (37.51). CD8+ T cells were added to the antibody-treated plates and cultured for 16 h. Robust GFP fluorescence was observed, indicative of T cell activation (Au-Yeung et al., 2014; Courtney et al., 2019; Moran et al., 2011), in T cells treated with the anti-CD3ε agonist (Fig. 1A). The fluorescence intensity of each cell was quantified to determine the proportion of GFP+ T cells present under each treatment condition (Fig. 1B). The expected trend was observed where the proportion of activated (GFP+) T cells declined as the concentration of agonist

decreased (Fig. 1CD). Little or no GFP+ cells could be detected in negative controls lacking anti-CD3ε agonist. The dose-response was determined by plotting GFP+ T cells versus anti-CD3ε agonist concentration. By incorporating an anti-CD28 agonist, we observed an apparent shift in the proportion of activated T cells caused by the anti-CD3ε agonist. The EC_{50} for activation was 2.5 μg/mL (95% confidence interval (CI) of 2.042 to 3.085) for CD3ε agonist alone, in comparison to an EC_{50} of 1.27 μg/mL (95% CI of 0.9802 to 1.739) for the combined anti-CD28 and anti-CD3ε agonistic antibodies.

Having established that activated T cells can be quantified by imaging cytometry using the Nur77-GFP reporter system, we sought to evaluate whether this system could be used in co-cultures. We therefore interrogated the relationship between the recognition of a tumor antigen (TA) by T cells and their capacity to execute cell-mediated cytotoxicity. Our goal was to establish a platform for the combined quantification of activated T cells and cancer cell death. We incorporated a non-secreted Ovalbumin variant (OVA) into MC38 adenocarcinoma cells by viral transduction to generate a clonal cell line (denoted MC38-OVA) (Supporting Information) (Diebold et al., 2001). The MC38 cell line is adherent and not readily amenable to flow cytometric analysis, making imaging cytometry an attractive alternative to evaluate the capacity of T cells to recognize and kill this widely utilized cell line. OT-I TCR transgenic mice were crossed with Nur77-GFP transgenic mice to combine the OVA-specific OT-I TCR with the Nur77-GFP reporter. Splenocytes were isolated from Nur77-GFP OT-I mice and OT-I T cells expanded by addition of an antigenic peptide and recombinant mouse IL-2 to generate CTLs (Fig. 2A). The expanded OT-I CTLs can recognize a peptide-MHC (pMHC) derived from the OVA protein incorporated into the MC38-OVA line, which acts as a model TA. The parental MC38 cell line should not be recognized by the OT-I TCR because it lacks the OVA antigen, and thus serves as a negative control to ensure cell death is antigen-specific. Our goal was to determine whether Nur77-GFP could be used to determine the relationship between the number of activated CTLs and killed cancer cells. We combined OT-I CTLs with MC38-OVA cells at different effector-to-target ratios (E:T). Co-cultures were incubated for 16 h and then stained with Hoechst dye to identify nucleated cells and propidium iodide (PI) to identify dead cells. The co-cultures were then analyzed by imaging cytometry. We observed robust induction of GFP when CTLs were co-cultured with MC38-OVA, but not the parental MC38 cell line, which lacks the OVA antigen. Distinct GFP+ and PI+ populations could be readily distinguished (Fig. 2BC). Consistent with the requirement for TA recognition prior to T cell-mediated killing of MC38-OVA, we observed a marked increase in PI+ MC38-OVA cells, but not the parental MC38. Moreover, the extent of cell death was proportional to the extent of activated (GFP+) CTLs. We evaluated over E:T that ranged from conditions where fewer than 1 in 10 cells were CTLs to where CTLs exceeded cancer cells by 5:1 (Fig. 2D). To determine the relationship between the number of MC38 killed and T cell activation, we determined the ratio of PI+ cells to activated (GFP+) CTLs (Fig. 2E). These observations revealed that potent CTL-mediated killing of MC38-OVA could be quantified at low E:T ratios (less than 1).

Having determined that the Nur77-GFP reporter provides a robust readout of activated CTLs co-cultured with cancer cells, we predicted it could also be used to identify the proportion of T cells that respond to a TA. We therefore evaluated T cell-cancer co-cultures that

contained heterogeneous lymphocyte populations: a mixture of T cells that recognize a TA and those that do not. We combined a fixed number of Nur77-GFP OT-I CTLs with splenocytes that would act as non-responsive “decoys”. A series of effector-to-decoy ratios was generated by combining increasing numbers of splenocytes with a fixed number of Nur77-GFP OT-I CTLs (Fig. 3A). These lymphocyte mixtures were then added to MC38 cells and cultured for 16 h. Co-cultures were stained with Hoechst and PI as described previously and quantification of PI+ and GFP+ cells performed by imaging cytometry. In co-cultures lacking a tumor antigen (MC38), we observed no cancer cell death and few GFP+ cells. However, presentation of a tumor antigen (MC38-OVA), allowed us to quantify comparable levels of GFP+ CTLs despite increasing numbers of unresponsive decoys (Fig. 3B). Similarly, the proportion of quantified PI+ MC38-OVA cells was also consistent across samples with increasing numbers of decoy cells (Fig. 3C).

Combined quantification of Nur77-GFP and cell-mediated cytotoxicity could be used to assess the effects of an inhibitor on T cell activation and a functional response. To test the feasibility of this approach, we evaluated the effects of a small molecule SRC family kinase inhibitor, PP2, because it inhibits the activity of LCK and FYN kinases (Hanke et al., 1996). These kinases are required for T cell activation because they phosphorylate the TCR complex and the ZAP-70 kinase. We treated our OT-I CTL co-cultures with a range of PP2 concentrations. An initial experiment revealed that PP2 caused a rapid decline in cell-mediated cytotoxicity (PI+) (Fig. 4A). We then evaluated a narrower range of PP2 dilutions and observed a decrease in activated (GFP+) CTLs with an IC_{50} of 2.724 (95% CI of 2.321 to 3.180). As anticipated, we observed a corresponding similar decrease in MC38-OVA cells that were killed (PI+) IC_{50} of 3.820 (95% CI of 2.99 to 7.90) (Fig. 4B).

4. Discussion

The development and characterization of immuno-oncology drugs and T cell-based therapies requires methods that can be used to evaluate them using cultured cells. Current methods to assess T cell activation ex vivo are typically performed separately from procedures used to assess functional readouts, such as T cell-mediated killing of cancer cells. Multiparameter flow cytometry is routinely used to analyze hallmarks of T cell activation but requires cellular suspensions that can restrict analysis of co-cultures that contain adherent cancer cells and is limited by throughput. We reasoned the Nur77-GFP reporter system could be combined with imaging cytometry to rapidly quantify activated T cells. We evaluated the utility of the Nur77-GFP reporter by imaging cytometry by determining the extent to which naïve T cells became activated following stimulation with a TCR agonistic antibody in the presence or absence of co-stimulation by a CD28 agonistic antibody. We also determined that Nur77-GFP became upregulated when CTLs were co-cultured with antigen-bearing MC38 cancer cells. The extent of CTL-mediated killing of cancer cells could be quantified by incorporating a readout of cell death. These combined readouts can be used to determine the effects of potential drug targets that influence TA recognition and T cell-mediated cancer cell death.

Sources of heterogeneity can affect the therapeutic potential of T cell-based therapies, such as CAR-T cells. Heterogeneity is known to arise from variable transduction efficiency and

phenotypic changes that occur during expansion procedures (Alizadeh et al., 2019; Gattinoni et al., 2005). Other sources of T cell heterogeneity can result when T cells are genetically modified, such as by CRISPR/Cas9 genome editing, which can produce mixed edited and unedited cells (Rupp et al., 2017). Genome editing procedures may also be used to reduce heterogeneity in modified T cells (Muller et al., 2021). An integrated readout of T cell activation combined with cancer cell death could be used to determine whether phenotypic differences that influence T cell activation result in altered T cell-mediated cytotoxicity. Our findings demonstrate that activated (GFP+) T cells in heterogeneous lymphocyte populations can be quantified to evaluate the relationship between responding TA-specific T cells and non-responsive lymphocytes, and the extent of cancer cell death. The described imaging cytometry platform could be combined with procedures used to incorporate alternative antigen recognition receptors, such as TA-specific TCRs, by genome engineering or viral transduction (Freen-van Heeren et al., 2020; Gomez-Eerland et al., 2014). Notable examples include modfied T cells specific for tumor antigens, such as MART-1 or Mesothelin (Morgan et al., 2006; Stromnes et al., 2015; Watanabe et al., 2018). To assess their function, humanized receptors can also be incorporated into mouse T cells (Yu et al., 2004; Zhong et al., 2010). By integrating readouts of T cell activation and cancer cell death, optimizations can be performed prior to in vivo testing. Alternatively, we anticipate that antigen-specific receptors can be combined with reporter systems, such as NFAT and IL-2 reporters, that have been incorporated into human cell lines, such as Jurkat T cells (Jutz et al., 2016; Shapiro et al., 1997).

The throughput of analysis is an important consideration for screening and testing procedures. Because imaging cytometry allowed us to directly analyze co-cultured cells, samples were labeled by direct addition of dyes followed by a brief incubation prior to being imaged. A single 96-well plate could be used to routinely assess 7 different effector-to-target ratios and controls. The imaging process and analysis could be performed in about 15 min per plate. As proof-of-principle, we evaluated a small molecule inhibitor of SRC family kinases, PP2. PP2 is known to inhibit TCR signaling by preventing LCK and FYN kinases from phosphorylating the TCR complex (Hanke et al., 1996). We could readily determine the concentration of PP2 required to inhibit T cell activation and T cell-mediated cytotoxicity. Because plates can be rapidly processed and imaged, this platform is amenable to analyses that sample a large swath of treatment conditions, such as those used to optimize T cell expansion (Kaartinen et al., 2017; Levine et al., 2017; Li and Kurlander, 2010). Although we evaluated a known inhibitor of CTL function (PP2), we anticipate our method can be extended to evaluate compounds that rescue T cell function. Co-cultures could be modified to incorporate inhibitory factors that suppress the capacity of CTLs to become activated and kill cancer cells. Based on the capacity to rescue CTL loss-of-function, phenotypic screens could then be conducted, or drug candidates evaluated. For example, target cells could be modified to express ligands known to engage immune checkpoints, such as PD-L1 (Freeman et al., 2000). Soluble factors that are known to be suppressive, such as TGFβ (Thomas and Massague, 2005), could also be incorporated to identify or test strategies that overcome T cell suppression.

Supplementary Material

Refer to Web version on PubMed Central for supplementary material.

Acknowledgements

This study was supported by: The Elsa U. Pardee Foundation (AHC), the V Foundation Scholar Award (AHC), the Pharmacological Sciences Training Program (T32GM140223) (CES), the Cancer Biology Training Program (T32CA009676) (MKC), and a Charles W. Edmunds Pharmacology Fellowship (YZ). This study was also supported by resources provided by the U-M Flow Cytometry Core and the U-M Rogel Cancer Center (P30CA046592). We thank Dr. Weiping Zou for providing the MC38 cell line.

Data availability

Data will be made available on request.

References

Alizadeh D, Wong RA, Yang X, Wang D, Pecoraro JR, Kuo CF, Aguilar B, Qi Y, Ann DK, Starr R, et al. , 2019. IL15 enhances CAR-T cell antitumor activity by reducing mTORC1 activity and preserving their stem cell memory phenotype. Cancer Immunol. Res 7, 759–772. 10.1158/2326-6066.CIR-18-0466. [PubMed: 30890531]

Ashouri JF, Weiss A, 2017. Endogenous Nur77 is a specific Indicator of antigen receptor signaling in human T and B cells. J. Immunol 198, 657–668. 10.4049/jimmunol.1601301. [PubMed: 27940659]

Au-Yeung BB, Zikherman J, Mueller JL, Ashouri JF, Matloubian M, Cheng DA, Chen Y, Shokat KM, Weiss A, 2014. A sharp T-cell antigen receptor signaling threshold for T-cell proliferation. Proc. Natl. Acad. Sci. U. S. A 111, E3679–E3688. 10.1073/pnas.1413726111. [PubMed: 25136127]

Au-Yeung BB, Smith GA, Mueller JL, Heyn CS, Jaszczak RG, Weiss A, Zikherman J, 2017. IL-2 modulates the TCR signaling threshold for CD8 but not CD4 T cell proliferation on a single-cell level. J. Immunol 198, 2445–2456. 10.4049/jimmunol.1601453. [PubMed: 28159902]

Caruso A, Licenziati S, Corulli M, Canaris AD, De Francesco MA, Fiorentini S, Peroni L, Fallacara F, Dima F, Balsari A, Turano A, 1997. Flow cytometric analysis of activation markers on stimulated T cells and their correlation with cell proliferation. Cytometry 27, 71–76. 10.1002/(sici)1097-0320(19970101)27:1<71::aid-cyto9>3.0.co;2-o. [PubMed: 9000587]

Chan LL, Lai N, Wang E, Smith T, Yang X, Lin B, 2011. A rapid detection method for apoptosis and necrosis measurement using the Cellometer imaging cytometry. Apoptosis 16, 1295–1303. 10.1007/s10495-011-0651-8. [PubMed: 21910006]

Chan LL, Wucherpfennig KW, de Andrade LF, 2019. Visualization and quantification of NK cell-mediated cytotoxicity over extended time periods by image cytometry. J. Immunol. Methods 469, 47–51. 10.1016/j.jim.2019.04.001. [PubMed: 30951701]

Chen DS, Mellman I, 2013. Oncology meets immunology: the cancer-immunity cycle. Immunity 39, 1–10. 10.1016/j.immuni.2013.07.012. [PubMed: 23890059]

Courtney AH, Lo WL, Weiss A, 2018. TCR signaling: mechanisms of initiation and propagation. Trends Biochem. Sci 43, 108–123. 10.1016/j.tibs.2017.11.008. [PubMed: 29269020]

Courtney AH, Shvets AA, Lu W, Griffante G, Mollenauer M, Horkova V, Lo WL, Yu S, Stepanek O, Chakraborty AK, Weiss A, 2019. CD45 functions as a signaling gatekeeper in T cells. Sci. Signal 12 10.1126/scisignal.aaw8151.

Davis MM, Bjorkman PJ, 1988. T-cell antigen receptor genes and T-cell recognition. Nature 334, 395–402. 10.1038/334395a0. [PubMed: 3043226]

Diebold SS, Cotten M, Koch N, Zenke M, 2001. MHC class II presentation of endogenously expressed antigens by transfected dendritic cells. Gene Ther. 8, 487–493. 10.1038/sj.gt.3301433. [PubMed: 11313828]

Freeman GJ, Long AJ, Iwai Y, Bourque K, Chernova T, Nishimura H, Fitz LJ, Malenkovich N, Okazaki T, Byrne MC, et al. , 2000. Engagement of the PD-1 immunoinhibitory receptor by a

novel B7 family member leads to negative regulation of lymphocyte activation. J. Exp. Med 192, 1027–1034. 10.1084/jem.192.7.1027. [PubMed: 11015443]

Freen-van Heeren JJ, Popovic B, Guislain A, Wolkers MC, 2020. Human T cells employ conserved AU-rich elements to fine-tune IFN-gamma production. Eur. J. Immunol 50, 949–958. 10.1002/eji.201948458. [PubMed: 32112565]

Gattinoni L, Klebanoff CA, Palmer DC, Wrzesinski C, Kerstann K, Yu Z, Finkelstein SE, Theoret MR, Rosenberg SA, Restifo NP, 2005. Acquisition of full effector function in vitro paradoxically impairs the in vivo antitumor efficacy of adoptively transferred CD8+ T cells. J. Clin. Invest 115, 1616–1626. 10.1172/JCI24480. [PubMed: 15931392]

Gomez-Eerland R, Nuijen B, Heemskerk B, van Rooij N, van den Berg JH, Beijnen JH, Uckert W, Kvistborg P, Schumacher TN, Haanen JB, Jorritsma A, 2014. Manufacture of gene-modified human T-cells with a memory stem/central memory phenotype. Hum. Gene Ther. Methods 25, 277–287. 10.1089/hgtb.2014.004. [PubMed: 25143008]

Hanke JH, Gardner JP, Dow RL, Changelian PS, Brissette WH, Weringer EJ, Pollok BA, Connelly PA, 1996. Discovery of a novel, potent, and Src family-selective tyrosine kinase inhibitor. Study of Lck- and FynT-dependent T cell activation. J. Biol. Chem 271, 695–701. 10.1074/jbc.271.2.695. [PubMed: 8557675]

Hogquist KA, Jameson SC, Heath WR, Howard JL, Bevan MJ, Carbone FR, 1994. T cell receptor antagonist peptides induce positive selection. Cell 76, 17–27. [PubMed: 8287475]

Jenkins MR, Tsun A, Stinchcombe JC, Griffiths GM, 2009. The strength of T cell receptor signal controls the polarization of cytotoxic machinery to the immunological synapse. Immunity 31, 621–631. 10.1016/j.immuni.2009.08.024. [PubMed: 19833087]

Jutz S, Leitner J, Schmetterer K, Doel-Perez I, Majdic O, GrabmeierPfistershammer K, Paster W, Huppa JB, Steinberger P, 2016. Assessment of costimulation and coinhibition in a triple parameter T cell reporter line: simultaneous measurement of NF-kappaB, NFAT and AP-1. J. Immunol. Methods 430, 10–20. 10.1016/j.jim.2016.01.007. [PubMed: 26780292]

Kaartinen T, Luostarinen A, Maliniemi P, Keto J, Arvas M, Belt H, Koponen J, Makinen PI, Loskog A, Mustjoki S, et al. , 2017. Low interleukin-2 concentration favors generation of early memory T cells over effector phenotypes during chimeric antigen receptor T-cell expansion. Cytotherapy 19, 1130. 10.1016/j.jcyt.2017.06.003. [PubMed: 28645733]

Korzeniewski C, Callewaert DM, 1983. An enzyme-release assay for natural cytotoxicity. J. Immunol. Methods 64, 313–320. 10.1016/0022-1759(83)90438-6. [PubMed: 6199426]

Levine BL, Miskin J, Wonnacott K, Keir C, 2017. Global manufacturing of CAR T cell therapy. Mol. Ther. Methods Clin. Dev 4, 92–101. 10.1016/j.omtm.2016.12.006. [PubMed: 28344995]

Li Y, Kurlander RJ, 2010. Comparison of anti-CD3 and anti-CD28-coated beads with soluble anti-CD3 for expanding human T cells: differing impact on CD8 T cell phenotype and responsiveness to restimulation. J. Transl. Med 8, 104. 10.1186/1479-5876-8-104. [PubMed: 20977748]

Maino VC, Suni MA, Ruitenberg JJ, 1995. Rapid flow cytometric method for measuring lymphocyte subset activation. Cytometry 20, 127–133. 10.1002/cyto.990200205. [PubMed: 7664623]

Maldini CR, Love AC, Tosh KW, Chan LL, Gayout K, Smith T, Riley JL, 2020. Characterization of CAR T cell expansion and cytotoxic potential during Ex Vivo manufacturing using image-based cytometry. J. Immunol. Methods 484–485, 112830. 10.1016/j.jim.2020.112830.

Miller RG, Dunkley M, 1974. Quantitative analysis of the 51Cr release cytotoxicity assay for cytotoxic lymphocytes. Cell. Immunol 14, 284–302. 10.1016/0008-8749(74)90212-3. [PubMed: 4219591]

Moran AE, Holzapfel KL, Xing Y, Cunningham NR, Maltzman JS, Punt J, Hogquist KA, 2011. T cell receptor signal strength in Treg and iNKT cell development demonstrated by a novel fluorescent reporter mouse. J. Exp. Med 208, 1279–1289. 10.1084/jem.20110308. [PubMed: 21606508]

Moran AE, Polesso F, Weinberg AD, 2016. Immunotherapy expands and maintains the function of high-affinity tumor-infiltrating CD8 T cells in situ. J. Immunol 197, 2509–2521. 10.4049/jimmunol.1502659. [PubMed: 27503208]

Morgan RA, Dudley ME, Wunderlich JR, Hughes MS, Yang JC, Sherry RM, Royal RE, Topalian SL, Kammula US, Restifo NP, et al. , 2006. Cancer regression in patients after transfer of genetically engineered lymphocytes. Science 314, 126–129. 10.1126/science.1129003. [PubMed: 16946036]

Muller TR, Jarosch S, Hammel M, Leube J, Grassmann S, Bernard B, Effenberger M, Andra I, Chaudhry MZ, Kauferle T, et al. , 2021. Targeted T cell receptor gene editing provides predictable T cell product function for immunotherapy. Cell Rep. Med 2, 100374 10.1016/j.xcrm.2021.100374. [PubMed: 34467251]

Oja AE, Piet B, van der Zwan D, Blaauwgeers H, Mensink M, de Kivit S, Borst J, Nolte MA, van Lier RAW, Stark R, Hombrink P, 2018. Functional heterogeneity of CD4(+) tumor-infiltrating lymphocytes with a resident memory phenotype in NSCLC. Front. Immunol 9, 2654. 10.3389/fimmu.2018.02654. [PubMed: 30505306]

Osborne BA, Smith SW, Liu ZG, McLaughlin KA, Grimm L, Schwartz LM, 1994. Identification of genes induced during apoptosis in T lymphocytes. Immunol. Rev 142, 301–320. 10.1111/j.1600-065x.1994.tb00894.x. [PubMed: 7698798]

Piriou L, Chilmonczyk S, Genetet N, Albina E, 2000. Design of a flow cytometric assay for the determination of natural killer and cytotoxic T-lymphocyte activity in human and in different animal species. Cytometry 41, 289–297. 10.1002/1097-0320(20001201)41:4<289::aid-cyto7>3.0.co;2-5. [PubMed: 11084614]

Piscopo NJ, Mueller KP, Das A, Hematti P, Murphy WL, Palecek SP, Capitini CM, Saha K, 2018. Bioengineering solutions for manufacturing challenges in CAR T cells. Biotechnol. J 13 10.1002/biot.201700095.

Root DE, Hacohen N, Hahn WC, Lander ES, Sabatini DM, 2006. Genome-scale loss-of-function screening with a lentiviral RNAi library. Nat. Methods 3, 715–719. 10.1038/nmeth924. [PubMed: 16929317]

Rupp LJ, Schumann K, Roybal KT, Gate RE, Ye CJ, Lim WA, Marson A, 2017. CRISPR/Cas9-mediated PD-1 disruption enhances anti-tumor efficacy of human chimeric antigen receptor T cells. Sci. Rep 7, 737. 10.1038/s41598-017-00462-8. [PubMed: 28389661]

Shapiro VS, Truitt KE, Imboden JB, Weiss A, 1997. CD28 mediates transcriptional upregulation of the interleukin-2 (IL-2) promoter through a composite element containing the CD28RE and NF-IL-2B AP-1 sites. Mol. Cell. Biol 17, 4051–4058. 10.1128/MCB.17.7.4051. [PubMed: 9199340]

Stromnes IM, Schmitt TM, Hulbert A, Brockenbrough JS, Nguyen H, Cuevas C, Dotson AM, Tan X, Hotes JL, Greenberg PD, Hingorani SR, 2015. T cells engineered against a native antigen can surmount immunologic and physical barriers to treat pancreatic ductal adenocarcinoma. Cancer Cell 28, 638–652. 10.1016/j.ccell.2015.09.022. [PubMed: 26525103]

Thomas DA, Massague J, 2005. TGF-beta directly targets cytotoxic T cell functions during tumor evasion of immune surveillance. Cancer Cell 8, 369–380. 10.1016/j.ccr.2005.10.012. [PubMed: 16286245]

Upadhaya S, Hubbard-Lucey VM, Yu JX, 2020. Immuno-oncology drug development forges on despite COVID-19. Nat. Rev. Drug Discov 19, 751–752. 10.1038/d41573-020-00166-1. [PubMed: 32948858]

Watanabe K, Luo Y, Da T, Guedan S, Ruella M, Scholler J, Keith B, Young RM, Engels B, Sorsa S, et al. , 2018. Pancreatic cancer therapy with combined mesothelin-redirected chimeric antigen receptor T cells and cytokine-armed oncolytic adenoviruses. JCI Insight 3. 10.1172/jci.insight.99573.

Yu Z, Theoret MR, Touloukian CE, Surman DR, Garman SC, Feigenbaum L, Baxter TK, Baker BM, Restifo NP, 2004. Poor immunogenicity of a self/tumor antigen derives from peptide-MHC-I instability and is independent of tolerance. J. Clin. Invest 114, 551–559. 10.1172/JCI21695. [PubMed: 15314692]

Zhong S, Malecek K, Perez-Garcia A, Krogsgaard M, 2010. Retroviral transduction of T-cell receptors in mouse T-cells. J. Vis. Exp 10.3791/2307.

Zikherman J, Parameswaran R, Weiss A, 2012. Endogenous antigen tunes the responsiveness of naive B cells but not T cells. Nature 489, 160–164. 10.1038/nature11311. [PubMed: 22902503]

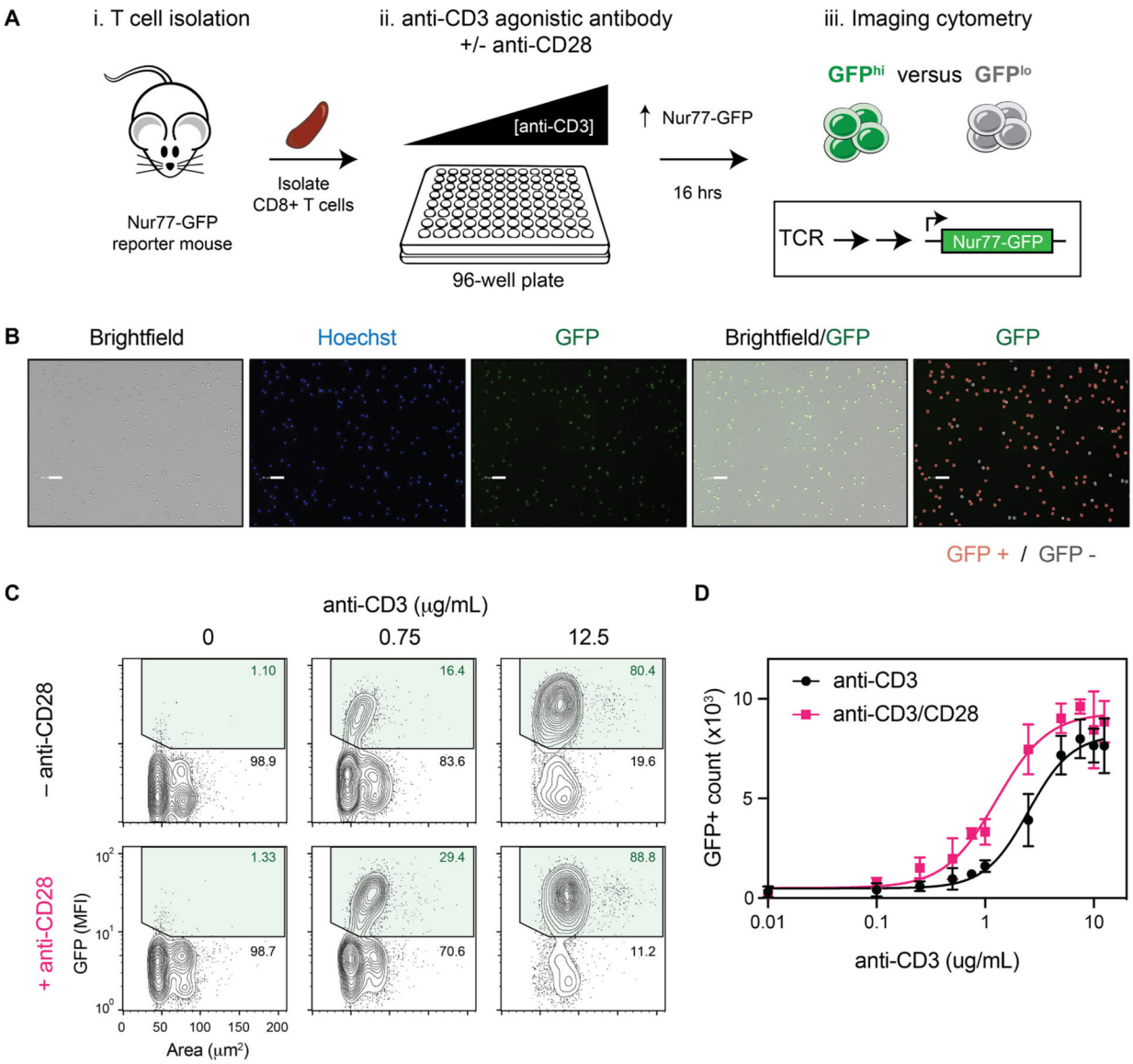

Fig. 1.

Quantification of T cell activation by imaging cytometry. (A) Schematic illustrating workflow for the quantification of activated T cells using the Nur77-GFP reporter. (B) Representative microscopy images of T cells treated with anti-CD3ε agonist and analysis of GFP+ and GFP− populations. Scale bars represent 50 μm. (C) Contour plots depicting GFP+ cells identified by imaging cytometry. (B–C) Data are representative of 4 independent replicates. (D) Quantification of GFP+ activated T cells over a range of anti-CD3ε concentrations in the presence or absence of an anti-CD28 co-stimulatory antibody. Four technical replicates were performed for each treatment condition. Error bars represent the standard deviation of three independent experiments (biological replicates, $n = 3$). Samples were compared by two-way ANOVA analysis (interaction, $p < 0.005$; sample and concentration, $p < 0.0001$).

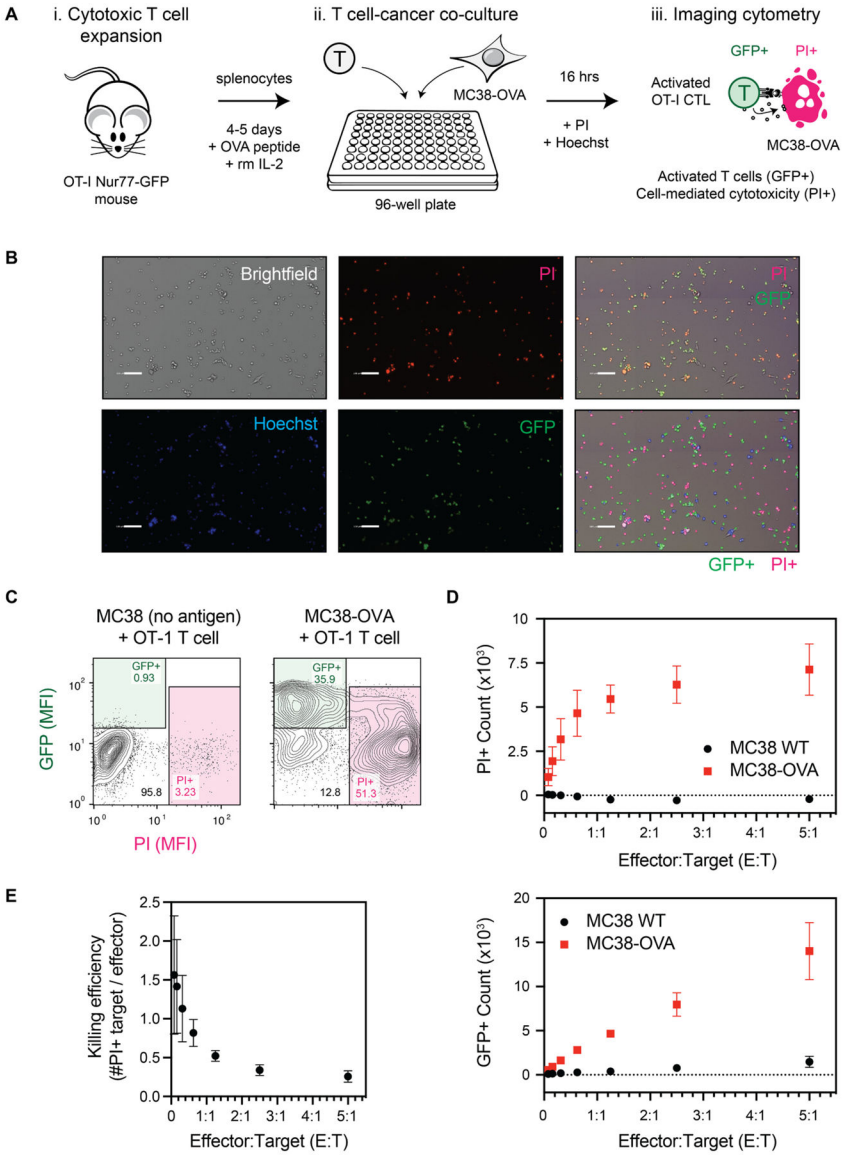

Fig. 2.

Quantification of CTL activation and T cell-mediated cytotoxicity by imaging cytometry. (A) Schematic illustrating the workflow for analysis of OT-I CTLs and MC38-OVA co-cultures using the Nur77-GFP reporter. (B) Representative images of OT-I CTLs co-cultured with antigen-bearing MC38-OVA cells, and analysis of GFP+ and PI+ populations. Scale bars represent 100 μm. (C) Contour plots depicting GFP+ and PI+ cells identified by imaging cytometry (E:T ratio of 1.25:1). (B–C) Data are representative of 4 independent replicates. (D) Quantification of activated T cells (GFP+) and dead cells (PI+) at several effector-to-target ratios (E:T). (E) The extent of MC38 cell death was plotted as a function of the number of CTLs in the co-culture. The E:T ratios tested were 5:1, 2.5:1, 1.25:1, 0.625:1, 0.313:1, 0.156, 0.078:1. Four technical replicates were performed for each treatment condition. Error bars represent the standard deviation from three independent experiments (biological replicates, $n = 3$).

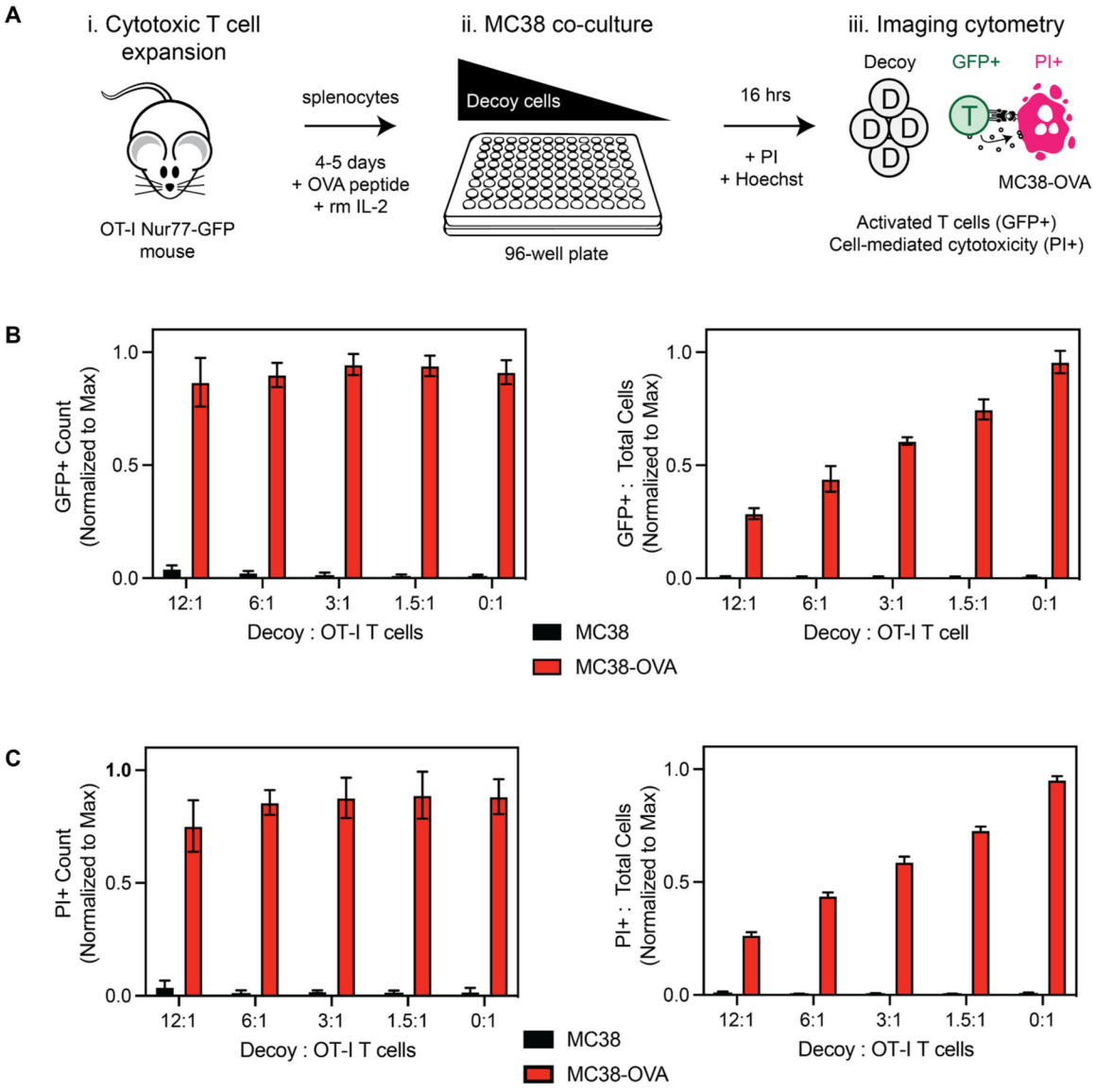

Fig. 3.

Quantification of activated CTLs in mixed lymphocyte-cancer co-cultures. (A) Schematic illustrating workflow for analysis of OT-I CTLs and MC38-OVA co-cultures using the Nur77-GFP reporter. Decoy splenocytes were incorporated into co-cultures to assess the proportion of activated CTLs. (B) Quantification of the number of activated T cells (GFP+) and the number of activated (GFP+) T cells to total cells. (C) Quantification of the number of dead cells (PI+) and the dead cells (PI+) to total cells. Three technical replicates were performed for each treatment condition. Error bars represent the standard deviation from three independent experiments (biological replicates, $n = 3$).

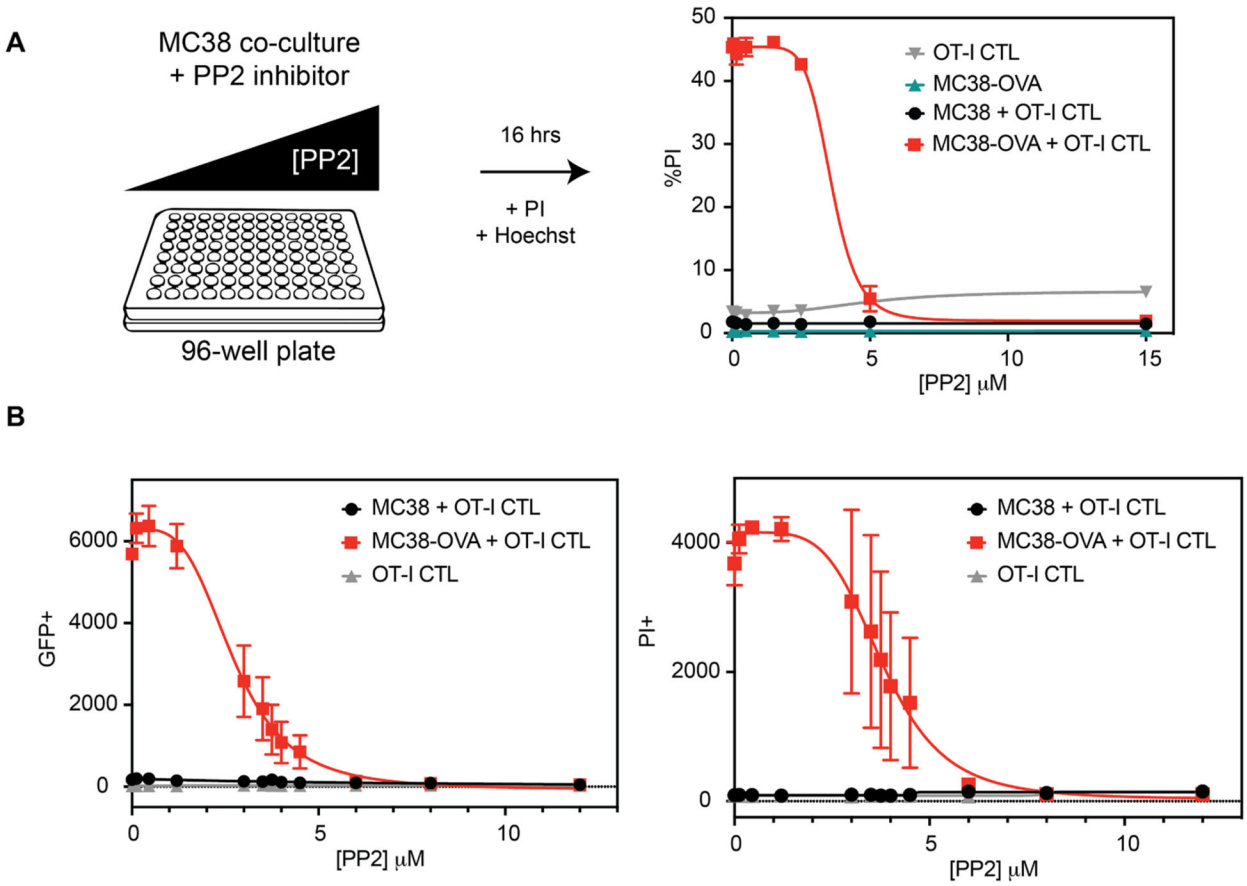

Fig. 4.

Analysis of TCR signaling inhibitor PP2. (A) Pilot experiment depicting PP2 dose-response. Error bars represent standard deviation of three technical replicates. (B) Dose-response of activated CTLs (GFP+) and proportion of dead cells (PI+) following treatment with PP2. Three technical replicates were performed for each treatment condition. Error bars represent the standard error of measurement from three independent experiments (biological replicates, n = 3).